

**Rotenone down-regulates HSPA8/hsc70 chaperone protein in vitro: a new possible toxic mechanism contributing to Parkinson's disease**

Gessica Sala<sup>1,6</sup>, Daniele Marinig<sup>1,2,6</sup>, Chiara Riva<sup>1,6</sup>, Alessandro Arosio<sup>1,2,6</sup>, Giovanni Stefanoni<sup>1,3</sup>, Laura Brighina<sup>3,6</sup>, Matteo Formenti<sup>4,5</sup>, Lilia Alberghina<sup>4,5,6</sup>, Anna Maria Colangelo<sup>4,5,6</sup>, Carlo Ferrarese<sup>1,3,6</sup>

<sup>1</sup>Lab. of Neurobiology, School of Medicine and Surgery, University of Milano-Bicocca; <sup>2</sup>PhD program in Neuroscience, University of Milano-Bicocca; <sup>3</sup>Dept. of Neurology, San Gerardo Hospital, Monza; <sup>4</sup>Lab. of Neuroscience R. Levi-Montalcini, Dept. of Biotechnology and Biosciences, University of Milano-Bicocca; <sup>5</sup>SYSBIO Centre of Systems Biology, University of Milano-Bicocca, Milano; <sup>6</sup>NeuroMI Milan Center for Neuroscience, University of Milano-Bicocca, Milano, Italy.

**Corresponding author:**

Gessica Sala, Ph.D.

Lab. of Neurobiology,

Milan Center for Neuroscience,

School of Medicine and Surgery,

University of Milano-Bicocca,

via Cadore, 48 – 20900 Monza (MB) – Italy

Phone: +39-02.6448.8128. Fax: +39-02.6448.8108.

E-mail: [gessica.sala@unimib.it](mailto:gessica.sala@unimib.it)

## **Abstract**

HSPA8/hsc70 (70-kDa heat shock cognate) chaperone protein exerts multiple protective roles. Beside its ability to confer to the cells a generic resistance against several metabolic stresses, it is also involved in at least two critical processes whose activity is essential in preventing Parkinson's disease (PD) pathology. As a matter of fact, hsc70 protein acts as the main carrier of chaperone-mediated autophagy (CMA), a selective catabolic pathway for alpha-synuclein, the main pathogenic protein that accumulates in degenerating dopaminergic neurons in PD. Furthermore, hsc70 efficiently fragments alpha-synuclein fibrils in vitro and promotes depolymerization into non-toxic alpha-synuclein monomers.

Considering that the mitochondrial complex I inhibitor rotenone, used to generate PD animal models, induces alpha-synuclein aggregation, this study was designed in order to verify whether rotenone exposure leads to hsc70 alteration possibly contributing to alpha-synuclein aggregation. To this aim, human SH-SY5Y neuroblastoma cells were treated with rotenone and hsc70 mRNA and protein expression were assessed; the effect of a generic oxidative stress donor, hydrogen peroxide, on hsc70 expression was also evaluated to verify the specificity of rotenone-induced hsc70 alterations. The effect of rotenone on hsc70 was also confirmed in primary mouse cortical neurons. As we confirmed a rotenone-induced autophagosome accumulation, the possible contribution of macroautophagy to rotenone-induced modulation of hsc70 was also explored. We demonstrated that rotenone, but not hydrogen peroxide, induced a significant reduction of hsc70 mRNA and protein expression. We also observed that the toxic effect of rotenone on alpha-synuclein levels was amplified when macroautophagy was inhibited, although rotenone-induced hsc70 reduction was independent from macroautophagy. These findings demonstrate the existence of a novel mechanism of rotenone toxicity mediated by hsc70 and indicate that dysfunction of both CMA and macroautophagy can synergistically exacerbate alpha-synuclein toxicity, suggesting that hsc70 up-regulation may represent a valuable therapeutic strategy for PD.

## **Keywords**

Heat shock cognate protein 70, rotenone, Parkinson's disease, autophagy

## 1. Introduction

HSPA8/hsc70 (70-kDa heat shock cognate) protein represents a constitutively expressed protein belonging to the heat shock protein 70 (hsp70) chaperone family (Liu et al., 2012). Hsc70 is mainly localized in the intracellular space, possesses a highly conserved aminoacid sequence and plays a critical role in a variety of cellular mechanisms including endocytosis, protein folding and degradation (Stricher et al., 2013).

Recent studies reported that hsc70 is able to confer to the cells resistance against metabolic stress, hyperthermia and oxidative challenges (Chong et al., 2013; Wang et al., 2013a). Furthermore, particularly relevant is the involvement of hsc70 protein in the autophagic pathway known as chaperone-mediated autophagy (CMA), a selective device for the degradation of aberrant proteins containing the consensus peptide sequence KFERQ, which are directly transported to the lysosomes by a translocation system constituted by specific carrier proteins including cytosolic hsc70. Hsc70 is also localized into the lysosomal lumen where it allows the translocation of the substrate protein across the lysosomal membrane (Cuervo and Wong, 2014). Dysfunction of the CMA pathway is known to be closely associated with Parkinson's disease (PD) (Alvarez-Erviti et al., 2010; Cuervo et al., 2004; Kabuta et al., 2008; Xilouri et al., 2009); in particular, a significant reduction of hsc70 levels was evidenced in the substantia nigra pars compacta and amygdala of PD brains (Alvarez-Erviti et al., 2010) and in lymphomonocytes obtained from sporadic PD patients (Sala et al., 2014). A significant downregulation of HSPA8/hsc70 was also observed in Alzheimer's disease post-mortem brain tissues (Silva et al., 2014), suggesting that loss of expression of this molecular chaperone should play a critical role in the neuronal death associated not only with PD but also with other neurodegenerative diseases.

Since a crucial pathogenic role in PD is recognized to be played by intraneuronal accumulation and aggregation of alpha-synuclein, the demonstration that CMA represents the main catabolic system for alpha-synuclein (Cuervo et al., 2004; Mak et al., 2010) has strengthened the link between CMA dysfunction and PD pathology. Further reinforcing the connection between hsc70 and PD, hsc70 has been demonstrated *in vitro* to bind to both soluble alpha-synuclein, slowing down its assembly into fibrils, and fibrillar form even with higher affinity (Pemberton et al., 2011; Pemberton and Melki, 2012), thus limiting the prion-like alpha-synuclein spreading known to amplify PD-associated neurodegeneration. Lastly, a very recent study demonstrated that HSPA8/hsc70 represents the main constituent of a disaggregase system that efficiently fragments alpha-synuclein fibrils *in vitro* into shorter fibrils and promotes their depolymerization into non-toxic alpha-synuclein monomers (Gao et al., 2015). These findings identify other protective mechanisms exerted by hsc70 against the cytotoxicity associated with alpha-synuclein aggregation and inter-neuronal propagation occurring in PD.

It is well known that exposure to rotenone, an inhibitor of the mitochondrial complex I, is able to reproduce PD pathology both in animal and cellular models, as indicated by the degeneration of nigrostriatal dopaminergic neurons and the formation in nigral neurons of alpha-synuclein-positive cytoplasmic inclusions (Betarbet et al., 2000; Gao et al., 2002;

Sherer et al., 2003), although with some important limitations (Höglinger et al., 2006). Considering that rotenone induces alpha-synuclein aggregation and that hsc70 has a disaggregant effect on alpha-synuclein, this study was designed in order to verify whether rotenone exposure leads to hsc70 alteration possibly contributing to alpha-synuclein aggregation. To this aim, human SH-SY5Y neuroblastoma cells were treated with rotenone and hsc70 mRNA and protein expression was assessed; the effect of a generic oxidative stress donor, hydrogen peroxide, on hsc70 expression was also evaluated to verify the specificity of rotenone-induced hsc70 alterations. The effect of rotenone on hsc70 was also confirmed in primary mouse cortical neurons. As we confirmed a rotenone-induced autophagosome accumulation, the possible contribution of macroautophagy to rotenone-induced modulation of hsc70 was also explored.

## **2. Material and methods**

### **2.1. Cell cultures**

Human neuroblastoma SH-SY5Y cells were grown in Dulbecco's modified Eagle's medium-F12 (EuroClone) supplemented with 10% fetal bovine serum (EuroClone), 100 U/mL penicillin (EuroClone), 100 µg/mL streptomycin (EuroClone) and 2 mM L-glutamine (EuroClone), at 37°C in an atmosphere of 5% CO<sub>2</sub> in air.

Cortical neurons were prepared as previously described (Cirillo et al., 2014). Animal experiments were carried out using protocols approved by the University of Milano-Bicocca Animal Care and Use Committee and by the Italian Ministry of Health (protocol number 14-2011). This study complies with the ARRIVE guidelines. Briefly, cortices were dissected from neonatal (P1-P2) C57BL/6J mice (Charles River Laboratories), washed in dissociation medium and digested by trypsin (0.15%) with deoxyribonuclease (DNase, 1 mg/ml, Sigma-Aldrich) at 37°C for 20 min. After mechanical dissociation, cells (1x10<sup>6</sup>/ml) were plated onto poly-D-lysine (1 mg/ml) coated dishes in Neurobasal medium (NB; Invitrogen) containing B27 (Invitrogen), bFGF 10 ng/ml (Invitrogen), glutamine 1mM (Sigma-Aldrich) and antibiotics (Sigma-Aldrich). Cultures were maintained at 37°C in 5% CO<sub>2</sub> and used after 8 days *in vitro* (DIV). To evaluate purity of cultures (99-99.5 %), cells were plated onto 12 mm poly-D-lysine coated coverslip (5000/well) and assessed by immunocytochemistry using anti-βIII-tubulin (Cell Signaling), as previously described (Cirillo et al., 2014). Neurons were imaged under a reversed microscope Olympus CX40 (X20) equipped with an Olympus camera.

### **2.2. Cytotoxicity assays**

The effect of rotenone or hydrogen peroxide on cell viability was assessed by the MTT assay based on reduction of the yellow tetrazolium salts (MTT) to the purple formazan by mitochondrial dehydrogenases. After exposure to rotenone (from 100 to 800 nM) or hydrogen peroxide (from 50 to 200 µM) for 24 hours, SH-SY5Y cells were incubated with 0.5 mg/ml MTT (Sigma-Aldrich) in standard medium for 45 min at 37°C in an atmosphere of 5% CO<sub>2</sub> in air. Similarly, cortical neurons (5000 cells/well) at DIV8 were treated with rotenone (from 100 to 800 nM) for 24 hours and incubated with MTT (0.5 mg/ml) for 4 hours. After cell solubilization with DMSO, absorbance was quantified (wavelength 570

nm) using a multi-mode microplate reader (FLUOstar Omega, BMG LABTECH) and cell viability expressed as % vs. vehicle-treated cells. Since rotenone affects mitochondrial function, rotenone-induced cell death was also evaluated with the Trypan blue exclusion test in order to independently confirm results obtained at MTT assay.

### **2.3. Whole-cell reactive oxygen species (ROS) levels**

The dye 2',7'-dichlorofluorescein diacetate (DCF-DA, Sigma-Aldrich) was used to quantify the levels of whole-cell ROS. After medium removal, cells were exposed to 10  $\mu$ M DCF-DA in Locke's buffer (154 mM NaCl, 5.6 mM KCl, 3.6 mM NaHCO<sub>3</sub>, 2.3 mM CaCl<sub>2</sub>, 5.6 mM glucose, 5 mM Hepes, 1.2 mM MgCl<sub>2</sub>, pH 7.4) for 45 min at 37°C in an atmosphere of 5% CO<sub>2</sub> in air. Cells were washed in Locke's buffer without glucose, harvested and lysed. Fluorescence units (FU) were quantified (excitation 488 nm, emission 525 nm) and related to the total protein content assessed using the method of Bradford.

### **2.4. RNA extraction and cDNA synthesis**

Total RNA was extracted using the RNeasy Mini kit (Qiagen), according to the manufacturer instructions. RNA concentration was determined spectrophotometrically at 260 nm. RNA (2000 ng) was retro-transcribed into cDNA using the SuperScript® VILO™ cDNA Synthesis Kit (Invitrogen) at the following conditions: 10 min at 25°C and 60 min at 42°C. The reaction was terminated at 85°C for 5 min and cDNAs stored at -20°C.

### **2.5. Real-time quantitative PCR (qPCR)**

cDNAs obtained from RNA (50 ng for hsc70 and 100 ng for alpha-synuclein) were amplified in triplicate in the ABI Prism 7500 HT Sequence Detection System (Applied Biosystems) using the Platinum® SYBR® Green qPCR SuperMix-UDG (Invitrogen) at the following conditions: 50°C for 2 min, 95°C for 10 min, 40 cycles of: 95°C for 15 sec, 60°C for 30 sec. The following primer pairs were used: human hsc70-F (CAGGTTTATGAAGGCGAGCGTGCC) and human hsc70-R (GGGTGCAGGAGGTATGCCTGTGA); human alpha-synuclein-F (GCAGCCACTGGCTTTGTCAA) and human alpha-synuclein-R (AGGATCCACAGGCATATCTTCCA); human beta-actin-F (TGTGGCATCCACGAACTAC) and human beta-actin-R (GGAGCAATGATCTTGATCTTCA); mouse hsc70-F (CCTCGGAAAGACCGTTACCA) and mouse hsc70-R (TTTGTTGCCTGTGCTGAGA); mouse beta-actin-F (GTCGAGTCGCGTCCACC) and mouse beta-actin-R (GTCATCCATGGCGAACTGGT). For relative quantification of each target vs. beta-actin mRNA, the comparative C<sub>T</sub> method was used as previously described (Sala et al., 2010).

### **2.6. Western blotting**

Cell pellets were lysed in cell extraction buffer (Invitrogen) supplemented with 1 mM PMSF and protease inhibitor cocktail (Sigma-Aldrich) and protein concentrations determined by Bradford's method. After denaturation, 10 and 30  $\mu$ g (for mouse and human hsc70, respectively), 30  $\mu$ g (for beclin-1) or 50  $\mu$ g (for LC3II and alpha-synuclein) proteins were separated by electrophoresis in 8% or 4-12% SDS-PAGE and transferred to nitrocellulose. Blots were blocked for 1 hour,

incubated overnight at 4°C with specific primary antibodies (hsc70 Abcam, 1:3,000 dilution, beclin-1 Cell Signaling, 1:1,000 dilution; LC3B Cell Signaling, 1:500 dilution; alpha-synuclein BD Biosciences, 1:1,000 dilution) and then with the HRP-linked anti-mouse or –rabbit IgG for 1 hour. Beta-actin (Sigma, 1:30,000 dilution) was used as internal standard. Signals were revealed by chemiluminescence, visualized on X-ray film and quantified by GS-690 Imaging Densitometer (Bio-Rad).

## **2.7. Statistical analysis**

All data are shown as mean  $\pm$  standard deviation (SD). Statistical analysis was performed using GraphPad Prism 4.0. Repeated measures ANOVA, followed by Tukey's multiple comparison test, was used to assess the significance of differences between groups.

## **3. Results**

Attenzione a “and/or”, perché “and” significa letteralmente che le cellule sono state trattate per 6h e per 24h consecutivamente, mentre il trattamento è per 6h o per 24h. Se troviamo un reviewer rompi-p..... e madrelingua, si infastidisce... Vedi poi il commento alla fine di 3.1

Io eviterei tanti piccoli sottoparagrafi perché spezzettano il discorso. Inoltre, la citotossicità di rotenone e H<sub>2</sub>O<sub>2</sub> non sono una novità né su neuroblastoma né su neuroni corticali, per cui sono irrilevanti come paragrafo a sé. Possono essere OK come cappello di studi preliminari. Io farei solo paragrafo 3.1 (che include attuali 3.1 + 3.2) con il titolo del paragrafo 3.2; paragrafo 3.2 (che include 3.3 + 3.4) con il titolo del paragrafo 3.4; paragrafo 3.3 su macroautophagy (attuale 3.5).

### **3.1. Cytotoxic and pro-oxidant effect of rotenone and hydrogen peroxide in human SH-SY5Y cells (sostituire col titolo del 3.2 e fare paragrafo unico)**

Preliminary experiments were carried out to establish rotenone and hydrogen peroxide concentrations able to evoke similar cytotoxic and pro-oxidant effects in SH-SY5Y cells. While rotenone is a specific mitochondrial complex I inhibitor that secondarily results in cell damage by promoting generation of peroxides, hydrogen peroxide is a well-known oxidative stress donor. Exposure for 24 hours to rotenone concentrations ranging from 100 to 800 nM or hydrogen peroxide (from 50 to 200  $\mu$ M) caused a dose-dependent cell death, as shown in Figure 1A. Whole-cell intracellular ROS production was also quantified as index of rotenone- or hydrogen peroxide-induced oxidative stress. Exposure for 24 hours to 200 or 400 nM rotenone caused a significant increase (65 and 90 %, respectively;  $p < 0.01$ ) of ROS production with respect to vehicle-treated cells (Figure 1B). Similarly, 24 hours treatment with hydrogen peroxide (50 or 100  $\mu$ M) resulted in a 30 ( $p < 0.05$ ) and 80 % ( $p < 0.01$ ) ROS increase (Figure 1B). Based on results derived from cytotoxicity studies, we decided to evaluate hsc70 gene and protein expression levels after treatment with rotenone or hydrogen peroxide at concentrations responsible for a mild to moderate cytotoxic effects. Therefore, SH-SY5Y cells were exposed to 200 and

400 nM rotenone or 50 and 100  $\mu$ M hydrogen peroxide for 6 and 24 hours. (Nella attuale disposizione di paragrafi, questa frase evidenziata andrebbe meglio come cappello al paragrafo 3.2)

### **3.2. Effect of rotenone and hydrogen peroxide on hsc70 mRNA and protein expression in human SH-SY5Y cells**

After treatment with rotenone for 6 or 24 hours, levels of mRNA encoding for hsc70 were quantified by real-time PCR. Relative quantification (RQ) of hsc70 normalized to beta-actin in SH-SY5Y is represented in f. Rotenone induced a significant dose- and time-dependent decrease of mRNA encoding for hsc70, as compared to vehicle-treated cells. Surprisingly, instead, western blot analyses showed that 6 hours treatment with rotenone (200 or 400 nM) resulted in a progressive increase of hsc70 protein levels, while prolonged incubation of SH-SY5Y cells with the same rotenone concentrations for 24 hours caused a dose-dependent reduction of hsc70 protein expression (Figure 2B-C).

Hsc70 expression was also assessed after exposure to hydrogen peroxide, used as paradigm of oxidative stress. No significant change in hsc70 mRNA and protein levels was observed after 24 hours exposure to 50 or 100  $\mu$ M hydrogen peroxide (Figure 3, togliere 24h dalla figura accanto alla [ ], il tempo lo si può dire solo nella legenda). No changes were observed in hsc70 gene and protein levels after 6 hours treatment with hydrogen peroxide (data not shown).

### **3.3. Cytotoxicity of rotenone in mouse cortical neurons (togliere questo titolo e mettere questa frase all'inizio del par 3.4)**

#### **3.2. Effect of rotenone on hsc70 mRNA and protein expression in mouse cortical neurons**

To validate the neurotoxic effect of rotenone on hsc70 expression, we used mouse cortical neurons. As shown in Figure 4A, exposure of cortical neurons to increasing concentrations of rotenone (100-800 nM) for 24 hours caused a dose-dependent cell death, while progressively increasing their loss of neuronal branched morphology (Figure 4B).

Hsc70 mRNA and protein levels in primary neurons challenged with 200-400 nM rotenone for 6 or 24 hours showed a trend similar to that observed in neuroblastoma cells, as indicated by the significant time- and dose-dependent reduction of hsc70 mRNA levels (Figure 5A). Similarly to SH-SY5Y cells, western blot analyses showed that 6 hours treatment with rotenone did not affect hsc70 protein levels, while exposure to rotenone (200-400 nM) for 24 hours caused a significant reduction of hsc70 protein expression (Figure 5B-C).

#### **3.5. Effect of macroautophagy inhibition on rotenone-induced hsc70 and alpha-synuclein modulation in SH-SY5Y cells**

Next, we examined whether rotenone induces macroautophagy in SH-SY5Y cells. To this end, expression of LC3II and beclin-1, two proteins typically used to monitor macroautophagy, were assessed in SH-SY5Y cells exposed to 100-400 nM rotenone for 24 hours. Western blot analysis revealed that rotenone induced a significant increase of LC3II, while no change in beclin-1 protein expression was observed in rotenone-treated cells (Figure 6A-B).

To explore a putative role for macroautophagy in rotenone-induced modulation of hsc70, hsc70 mRNA and protein levels were assessed in presence of a specific macroautophagy inhibitor, 3-methyladenine (3-MA, 5mM, 1 hour before rotenone treatment). We found that 3-MA alone did not affect hsc70 mRNA and protein levels and did not modify the reduction of hsc70 mRNA (Figure 7A) and protein levels caused by rotenone exposure (Figure 7B-C). Furthermore, the effect of macroautophagy inhibition was also verified on alpha-synuclein expression during rotenone toxicity. Treatment with 3-MA resulted in a significant reduction (-37%,  $p<0.05$ ) of alpha-synuclein mRNA levels (Figure 7A) and increase of its protein levels (+41%,  $p<0.05$ ) (Figure 7B-C). As previously reported (Sala et al., 2013), exposure to rotenone caused an increase of alpha-synuclein mRNA and protein levels and, interestingly, macroautophagy inhibition resulted in a further increase of alpha-synuclein mRNA (+42% vs. rotenone-treated cells,  $p<0.05$ ) and protein (+49% vs. rotenone-treated cells,  $p<0.05$ ) levels (Figure 7).

#### 4. Discussion

Based on knowledge that hsc70 is a chaperone protein endowed with a critical role in several intracellular mechanisms known to be closely associated with PD, the aim of this study was to establish the existence of a possible modulation of hsc70 following exposure to PD-related stimuli. No previous study specifically explored the effect of rotenone on HSPA8/hsc70 chaperone protein in neuronal cells, although a reduction of the stress inducible hsp70 has been previously described in rotenone-treated rats (Sonia Angeline et al., 2012). Therefore, we assessed hsc70 mRNA and protein expression after mitochondrial inhibition by rotenone (a well-known inhibitor of the mitochondrial complex I) and oxidative stress, two major pathogenic mechanisms contributing to the loss of dopaminergic neurons in PD (Jenner and Olanow, 1998; Schapira et al., 1998). To this purpose, we used human neuroblastoma SH-SY5Y cells, a neuron-like cell line expressing dopaminergic markers and widely used to study PD pathomechanisms, and primary mouse cortical cultures, representing a neuronal population affected in late-stage PD. Maintaining proper levels of hsc70 appears fundamental for at least three processes whose dysfunction is known to lead to PD; as a matter of fact, hsc70 i) is required for the physiological activity of the CMA pathway, being hsc70 the principal carrier protein of CMA also essential to allow the entry of substrates into the lysosomal lumen (Cuervo and Wong, 2014); ii) it also cooperates to confer resistance against different metabolic cellular stresses (Chong et al., 2013; Wang et al., 2013a); iii) it prevents alpha-synuclein deposition and propagation through the binding to both soluble and fibrillar forms (Pemberton et al., 2011; Pemberton and Melki, 2012) and efficiently fragments alpha-synuclein fibrils *in vitro* into shorter fibrils and promotes depolymerization into non-toxic alpha-synuclein monomers (Gao et al., 2015).

Based on these considerations, we exposed SH-SY5Y cells to different concentrations of rotenone for 6 and 24 hours and we measured the effects of this treatment on hsc70 expression. Interestingly, we found that rotenone determined a dose- and time-dependent reduction of hsc70 mRNA levels, together with an initial (6 hours) increase of hsc70 protein levels



followed by a dose-dependent reduction after 24 hours rotenone exposure (Figure 2). These findings are in agreement with the knowledge that, under stress conditions, cells respond by upregulating the expression of molecular chaperones, which help to reverse stress-induced protein misfolding (Liu et al., 2012). These observations were confirmed in primary cortical neurons, which showed the same trend of hsc70 mRNA and protein levels when challenged with rotenone at the same concentrations and times (Figure 5).

We then compared the effect of the mitochondrial inhibitor rotenone, which also causes oxidative stress, versus the oxidative stress donor hydrogen peroxide. It was noteworthy to observe that concentrations of rotenone and hydrogen peroxide that caused similar cytotoxicity and intracellular ROS raise in SH-SY5Y cells differently affected hsc70 expression. In fact, while rotenone significantly reduced hsc70 gene expression (Figure 2A), hydrogen peroxide did not affect hsc70 mRNA and protein levels (Figure 3). These data suggest that mechanisms used by rotenone to reduce hsc70 expression may involve mitochondrial inhibition, but they are not directly linked to increased oxidative stress. Rather, it is conceivable that the effect of rotenone on hsc70 expression might be directly or indirectly linked to decreased mitochondrial bioenergetics, a primary outcome of mitochondrial complex I inhibition, leading to decreased ATP levels and induction of macroautophagy. Indeed, we found that treatment of SH-SY5Y cells with rotenone for 24 hours caused an increase of LC3-II levels, while leaving unchanged beclin-1 expression (Figure 6), in line with the rotenone-induced autophagosome accumulation already observed in these cells (Mader et al., 2012). Although we did not perform a complete study with specific pharmacological inhibitors of the autophagic steps, these data are indicative of a block of the autophagic flux caused by rotenone, as also previously reported in both *in vitro* and *in vivo* studies (Giordano et al., 2014; Mader et al., 2012; Wu et al., 2015).

Using a specific inhibitor of macroautophagy, we demonstrated that macroautophagy inhibition did not influence hsc70 expression, as evidenced by the similar rotenone-induced reduction in mRNA and protein hsc70 levels observed in the presence or absence of 3-MA (Figure 7); we found that macroautophagy inhibition by 3-MA did not modify *per se* hsc70 mRNA and protein levels under basal conditions. Based on knowledge that macroautophagy participates, together with CMA, to alpha-synuclein degradation (Webb et al., 2003), through macroautophagy inhibition, we also explored the specific contribution of CMA in the accumulation of alpha-synuclein caused by rotenone, as previously demonstrated in both *in vivo* and *in vitro* models (Betarbet et al., 2006; Betarbet et al., 2000; Sala et al., 2013).

Interestingly, we observed that macroautophagy inhibition by 3-MA was able to cause a significant increase of alpha-synuclein protein levels (Figure 7B-C), according to the knowledge that this protein is physiologically partially degraded by this pathway. Accumulation of alpha-synuclein protein (Figure 7B) could represent an inhibitory feedback responsible for the decrease of alpha-synuclein synthesis, as indicated by the reduction of mRNA levels in presence of 3-MA (Figure 7A). The increase of alpha-synuclein mRNA and protein levels induced by rotenone was further enhanced by

macroautophagy inhibition, which likely renders cells more susceptible to rotenone toxicity, thus confirming the need of a proper activity of both CMA and macroautophagy for maintaining the cellular homeostasis.

## **5. Conclusions**

The main finding of this study is the demonstration that constitutively expressed HSPA8/hsc70 chaperone protein represents a new intracellular targets of rotenone toxicity. This finding implies the existence of an adjunctive toxic mechanism of rotenone possibly contributing to PD pathogenesis and worthy of study in the attempt of identifying new therapeutic targets for the disease. Further studies exploring the molecular mechanisms responsible for rotenone-induced hsc70 reduction are needed, including the possible involvement of specific microRNA deregulation already reported to be associated with hsc70 reduction in PD (Alvarez-Erviti et al., 2013; Wang et al., 2013b).

## **Acknowledgements**

This work was carried out within the framework of the Ivascomar project, Cluster Tecnologico Nazionale Scienze della Vita ALISEI, Italian Ministry of Research (MIUR, to CF and AMC). This work was also supported by MIUR grants (PRIN2007 to AMC; SYSBIONET-Italian ROADMAP ESFRI Infrastructures to LA and AMC) and Associazione Levi-Montalcini (fellowships to MF).

## **Conflict of interest**

This manuscript is not under consideration for publication elsewhere and is free of any conflict of interest or financial implications.

## Figure legends

**Figure 1. (A) Cytotoxicity studies.** Cell viability was assessed by MTT assay after 24 hours exposure to 100-800 nM rotenone and 50-200  $\mu$ M hydrogen peroxide ( $H_2O_2$ ). Values are expressed as % vs. vehicle. N=6, repeated measures ANOVA test, followed by Tukey's post-test; \*  $p<0.05$ , \*\*  $p<0.01$  vs. vehicle. **(B) Whole-cell intracellular ROS production.** The effect on ROS production of 24 hours exposure to 200-400 nM rotenone or 50-100  $\mu$ M hydrogen peroxide ( $H_2O_2$ ) was shown and expressed as % vs. vehicle of dichlorofluorescein fluorescence units (DCF FU) normalized to protein content. N=4, repeated measures ANOVA test, followed by Tukey's post-test; \*  $p<0.05$ , \*\*  $p<0.01$  vs. vehicle.

**Figure 2. Effect of rotenone treatment on hsc70 mRNA and protein levels in human SH-SY5Y cells.** **(A)** Relative quantification (RQ) of hsc70 mRNA levels after treatment with rotenone (200-400 nM) for 6 or 24 hours. Hsc70 mRNA levels were calculated as ratio to beta-actin and expressed as -fold change vs. vehicle (RQ = 1). **(B)** Hsc70 protein levels normalized by beta-actin and expressed as % vs. vehicle. **(C)** Representative Western blot image showing the effect of 6 or 24 hours rotenone exposure on hsc70 protein expression. Immunoreactivity of beta-actin, used as internal standard, was also shown. N=10, repeated measures ANOVA test, followed by Tukey's post-test; \*  $p<0.05$ , \*\*  $p<0.01$  vs. vehicle.

**Figure 3. Effect of hydrogen peroxide ( $H_2O_2$ ) treatment on hsc70 mRNA and protein levels in human SH-SY5Y cells.** **(A)** Relative quantification (RQ) of hsc70 mRNA levels calculated as ratio to beta-actin and expressed as -fold change vs. vehicle (RQ = 1). **(B)** Hsc70 protein levels, expressed as % vs. vehicle of the ratio between hsc70 and beta-actin optical density. **(C)** Representative Western blot image showing the effect of 24 hours  $H_2O_2$  exposure on hsc70 protein expression. The immunoreactivity of beta-actin, used as internal standard, was also shown. N=10, repeated measures ANOVA test, followed by Tukey's post-test; \*  $p<0.05$  vs. vehicle.

**Figure 4. Survival of mouse cortical neurons exposed to rotenone for 24 hours.** **A.** Cell viability was assessed by MTT assay after 24 hours exposure to 100-800 nM rotenone. Values, expressed as % vs. vehicle, are the mean  $\pm$  SD of two separate experiments, each including five separate samples for each condition. \*  $p<0.05$ , \*\*  $p<0.01$  vs. vehicle; ANOVA test, followed by Dunnett's multiple comparisons test. **B.** Representative images of cortical neurons exposed for 24 hours to rotenone at the indicated concentrations. Neurons were imaged under a reversed microscope Olympus CX40 (X20) equipped with an Olympus camera.

**Figure 5. Effect of rotenone treatment on hsc70 mRNA and protein levels in mouse cortical neurons.** **A.** Relative quantification (RQ) of hsc70 mRNA levels after treatment with rotenone (200-400 nM) for 6 or 24 hours. Hsc70 mRNA content was calculated as ratio to beta-actin and expressed as -fold change vs. vehicle (RQ = 1). **B.** Hsc70 protein levels normalized by beta-actin and expressed as % vs. vehicle. **C.** Representative western blot image showing the effect of 6

or 24 hours rotenone exposure on hsc70 protein expression. Immunoreactivity of beta-actin, used as internal standard, was also shown. N=4, repeated measures ANOVA test, followed by Tukey's post-test; \* p<0.05, \*\* p<0.01 vs. vehicle.

**Figure 6. Effect of rotenone on macroautophagy.** **A.** LC3II and beclin-1 protein levels after treatment with rotenone (100-400 nM) for 24 hours. Hsc70 mRNA content was , expressed as % vs. vehicle of the ratio between target protein and beta-actin optical density. **B.** Representative western blot image showing the effect of rotenone treatment for 24 hours on LC3II and beclin-1 protein expression. Immunoreactivity of beta-actin, used as internal standard, was also shown. N=6, repeated measures ANOVA test, followed by Tukey's post-test; \* p<0.05, \*\* p<0.01 vs. vehicle.

**Figure 7. Effect of macroautophagy inhibition on rotenone-induced modulation of hsc70 and alpha-synuclein expression.** 3-methyladenine (3-MA, 5mM) was used to inhibit macroautophagy and administered 1 hour before rotenone treatment (200 nM, 24 hours). **A.** Relative quantification (RQ) of hsc70 and alpha-synuclein (asyn) mRNA levels calculated as ratio to beta-actin and expressed as -fold change vs. vehicle (RQ = 1). **B.** Hsc70 and asyn protein levels, expressed as % vs. vehicle of the ratio between target proteins and beta-actin optical density. **C.** Representative western blot image showing the effect of rotenone, 3-MA or rot/3-MA co-treatment on hsc70 and asyn protein expression. Immunoreactivity of beta-actin, used as internal standard, was also shown. N=3, repeated measures ANOVA test, followed by Tukey's post-test; \* p<0.05, \*\* p<0.01 vs. vehicle; § p<0.05 vs. rotenone-treated cells.

## References

- Alvarez-Erviti, L., M. C. Rodriguez-Oroz, J. M. Cooper, C. Caballero, I. Ferrer, J. A. Obeso, and A. H. Schapira, 2010, Chaperone-mediated autophagy markers in Parkinson disease brains: *Arch Neurol*, v. 67, p. 1464-72.
- Alvarez-Erviti, L., Y. Seow, A. H. Schapira, M. C. Rodriguez-Oroz, J. A. Obeso, and J. M. Cooper, 2013, Influence of microRNA deregulation on chaperone-mediated autophagy and  $\alpha$ -synuclein pathology in Parkinson's disease: *Cell Death Dis*, v. 4, p. e545.
- Betarbet, R., R. M. Canet-Aviles, T. B. Sherer, P. G. Mastroberardino, C. McLendon, J. H. Kim, S. Lund, H. M. Na, G. Taylor, N. F. Bence, R. Kopito, B. B. Seo, T. Yagi, A. Yagi, G. Klinefelter, M. R. Cookson, and J. T. Greenamyre, 2006, Intersecting pathways to neurodegeneration in Parkinson's disease: effects of the pesticide rotenone on DJ-1, alpha-synuclein, and the ubiquitin-proteasome system: *Neurobiol Dis*, v. 22, p. 404-20.
- Betarbet, R., T. B. Sherer, G. MacKenzie, M. Garcia-Osuna, A. V. Panov, and J. T. Greenamyre, 2000, Chronic systemic pesticide exposure reproduces features of Parkinson's disease: *Nat Neurosci*, v. 3, p. 1301-6.
- Chau, K. Y., H. L. Ching, A. H. Schapira, and J. M. Cooper, 2009, Relationship between alpha synuclein phosphorylation, proteasomal inhibition and cell death: relevance to Parkinson's disease pathogenesis: *J Neurochem*, v. 110, p. 1005-13.
- Chong, K. Y., C. C. Lai, and C. Y. Su, 2013, Inducible and constitutive HSP70s confer synergistic resistance against metabolic challenges: *Biochem Biophys Res Commun*, v. 430, p. 774-9.
- Cirillo, G., A. M. Colangelo, M. Berbenni, V. M. Ippolito, C. De Luca, F. Verdesca, L. Savarese, L. Alberghina, N. Maggio, and M. Papa, 2014, Purinergic Modulation of Spinal Neuroglial Maladaptive Plasticity Following Peripheral Nerve Injury: *Mol Neurobiol*.
- Cuervo, A. M., L. Stefanis, R. Fredenburg, P. T. Lansbury, and D. Sulzer, 2004, Impaired degradation of mutant alpha-synuclein by chaperone-mediated autophagy: *Science*, v. 305, p. 1292-5.
- Cuervo, A. M., and E. Wong, 2014, Chaperone-mediated autophagy: roles in disease and aging: *Cell Res*, v. 24, p. 92-104.
- Gao, H. M., J. S. Hong, W. Zhang, and B. Liu, 2002, Distinct role for microglia in rotenone-induced degeneration of dopaminergic neurons: *J Neurosci*, v. 22, p. 782-90.
- Gao, X., M. Carroni, C. Nussbaum-Krammer, A. Mogk, N. B. Nillegoda, A. Szlachcic, D. L. Guilbride, H. R. Saibil, M. P. Mayer, and B. Bukau, 2015, Human Hsp70 Disaggregase Reverses Parkinson's-Linked  $\alpha$ -Synuclein Amyloid Fibrils: *Mol Cell*, v. 59, p. 781-93.
- Giordano, S., M. Dodson, S. Ravi, M. Redmann, X. Ouyang, V. M. Darley Usmar, and J. Zhang, 2014, Bioenergetic adaptation in response to autophagy regulators during rotenone exposure: *J Neurochem*, v. 131, p. 625-33.
- Höglinger, G. U., W. H. Oertel, and E. C. Hirsch, 2006, The rotenone model of parkinsonism--the five years inspection: *J Neural Transm Suppl*, p. 269-72.
- Jenner, P., and C. W. Olanow, 1998, Understanding cell death in Parkinson's disease: *Ann Neurol*, v. 44, p. S72-84.
- Kabuta, T., A. Furuta, S. Aoki, K. Furuta, and K. Wada, 2008, Aberrant interaction between Parkinson disease-associated mutant UCH-L1 and the lysosomal receptor for chaperone-mediated autophagy: *J Biol Chem*, v. 283, p. 23731-8.
- Liu, T., C. K. Daniels, and S. Cao, 2012, Comprehensive review on the HSC70 functions, interactions with related molecules and involvement in clinical diseases and therapeutic potential: *Pharmacol Ther*, v. 136, p. 354-74.
- Mader, B. J., V. N. Pivtoraiko, H. M. Flipppo, B. J. Klocke, K. A. Roth, L. R. Mangieri, and J. J. Shacka, 2012, Rotenone inhibits autophagic flux prior to inducing cell death: *ACS Chem Neurosci*, v. 3, p. 1063-72.
- Mak, S. K., A. L. McCormack, A. B. Manning-Bog, A. M. Cuervo, and D. A. Di Monte, 2010, Lysosomal degradation of alpha-synuclein in vivo: *J Biol Chem*, v. 285, p. 13621-9.

- Pemberton, S., K. Madiona, L. Pieri, M. Kabani, L. Bousset, and R. Melki, 2011, Hsc70 protein interaction with soluble and fibrillar alpha-synuclein: *J Biol Chem*, v. 286, p. 34690-9.
- Pemberton, S., and R. Melki, 2012, The interaction of Hsc70 protein with fibrillar  $\alpha$ -Synuclein and its therapeutic potential in Parkinson's disease: *Commun Integr Biol*, v. 5, p. 94-5.
- Polymeropoulos, M. H., C. Lavedan, E. Leroy, S. E. Ide, A. Dehejia, A. Dutra, B. Pike, H. Root, J. Rubenstein, R. Boyer, E. S. Stenroos, S. Chandrasekharappa, A. Athanassiadou, T. Papapetropoulos, W. G. Johnson, A. M. Lazzarini, R. C. Duvoisin, G. Di Iorio, L. I. Golbe, and R. L. Nussbaum, 1997, Mutation in the alpha-synuclein gene identified in families with Parkinson's disease: *Science*, v. 276, p. 2045-7.
- Sala, G., A. Arosio, G. Stefanoni, L. Melchionda, C. Riva, D. Marinig, L. Brighina, and C. Ferrarese, 2013, Rotenone upregulates alpha-synuclein and myocyte enhancer factor 2D independently from lysosomal degradation inhibition: *Biomed Res Int*, v. 2013, p. 846725.
- Sala, G., L. Brighina, E. Saracchi, S. Fermi, C. Riva, V. Carozza, M. Pirovano, and C. Ferrarese, 2010, Vesicular monoamine transporter 2 mRNA levels are reduced in platelets from patients with Parkinson's disease: *J Neural Transm*, v. 117, p. 1093-8.
- Sala, G., G. Stefanoni, A. Arosio, C. Riva, L. Melchionda, E. Saracchi, S. Fermi, L. Brighina, and C. Ferrarese, 2014, Reduced expression of the chaperone-mediated autophagy carrier hsc70 protein in lymphomonocytes of patients with Parkinson's disease: *Brain Res*, v. 1546, p. 46-52.
- Schapira, A. H., M. Gu, J. W. Taanman, S. J. Tabrizi, T. Seaton, M. Cleeter, and J. M. Cooper, 1998, Mitochondria in the etiology and pathogenesis of Parkinson's disease: *Ann Neurol*, v. 44, p. S89-98.
- Sherer, T. B., J. H. Kim, R. Betarbet, and J. T. Greenamyre, 2003, Subcutaneous rotenone exposure causes highly selective dopaminergic degeneration and alpha-synuclein aggregation: *Exp Neurol*, v. 179, p. 9-16.
- Silva, P. N., T. K. Furuya, I. L. Braga, L. T. Rasmussen, R. W. Labio, P. H. Bertolucci, E. S. Chen, G. Turecki, N. Mechawar, S. L. Payão, J. Mill, and M. C. Smith, 2014, Analysis of HSPA8 and HSPA9 mRNA expression and promoter methylation in the brain and blood of Alzheimer's disease patients: *J Alzheimers Dis*, v. 38, p. 165-70.
- Singleton, A. B., M. Farrer, J. Johnson, A. Singleton, S. Hague, J. Kachergus, M. Hulihan, T. Peuralinna, A. Dutra, R. Nussbaum, S. Lincoln, A. Crawley, M. Hanson, D. Maraganore, C. Adler, M. R. Cookson, M. Muentner, M. Baptista, D. Miller, J. Blancato, J. Hardy, and K. Gwinn-Hardy, 2003, alpha-Synuclein locus triplication causes Parkinson's disease: *Science*, v. 302, p. 841.
- Sonia Angeline, M., P. Chaterjee, K. Anand, R. K. Ambasta, and P. Kumar, 2012, Rotenone-induced parkinsonism elicits behavioral impairments and differential expression of parkin, heat shock proteins and caspases in the rat: *Neuroscience*, v. 220, p. 291-301.
- Stricher, F., C. Macri, M. Ruff, and S. Muller, 2013, HSPA8/HSC70 chaperone protein: structure, function, and chemical targeting: *Autophagy*, v. 9, p. 1937-54.
- Wang, B. S., Y. Yang, H. Yang, Y. Z. Liu, J. J. Hao, Y. Zhang, Z. Z. Shi, X. M. Jia, Q. M. Zhan, and M. R. Wang, 2013a, PKC $\iota$  counteracts oxidative stress by regulating Hsc70 in an esophageal cancer cell line: *Cell Stress Chaperones*, v. 18, p. 359-66.
- Wang, Q., W. Hu, M. Lei, Y. Wang, B. Yan, J. Liu, R. Zhang, and Y. Jin, 2013b, MiR-17-5p impairs trafficking of H-ERG K<sup>+</sup> channel protein by targeting multiple er stress-related chaperones during chronic oxidative stress: *PLoS One*, v. 8, p. e84984.
- Webb, J. L., B. Ravikumar, J. Atkins, J. N. Skepper, and D. C. Rubinsztein, 2003, Alpha-Synuclein is degraded by both autophagy and the proteasome: *J Biol Chem*, v. 278, p. 25009-13.
- Wu, F., H. D. Xu, J. J. Guan, Y. S. Hou, J. H. Gu, X. C. Zhen, and Z. H. Qin, 2015, Rotenone impairs autophagic flux and lysosomal functions in Parkinson's disease: *Neuroscience*, v. 284, p. 900-11.

Xilouri, M., T. Vogiatzi, K. Vekrellis, D. Park, and L. Stefanis, 2009, Abberant alpha-synuclein confers toxicity to neurons in part through inhibition of chaperone-mediated autophagy: PLoS One, v. 4, p. e5515.

Figure 1

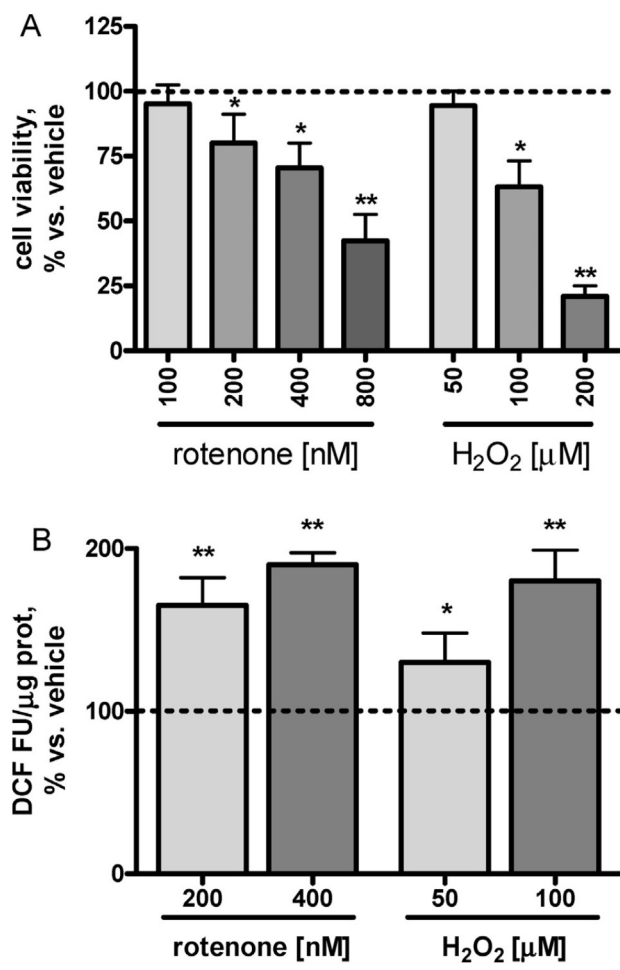




Figure 2

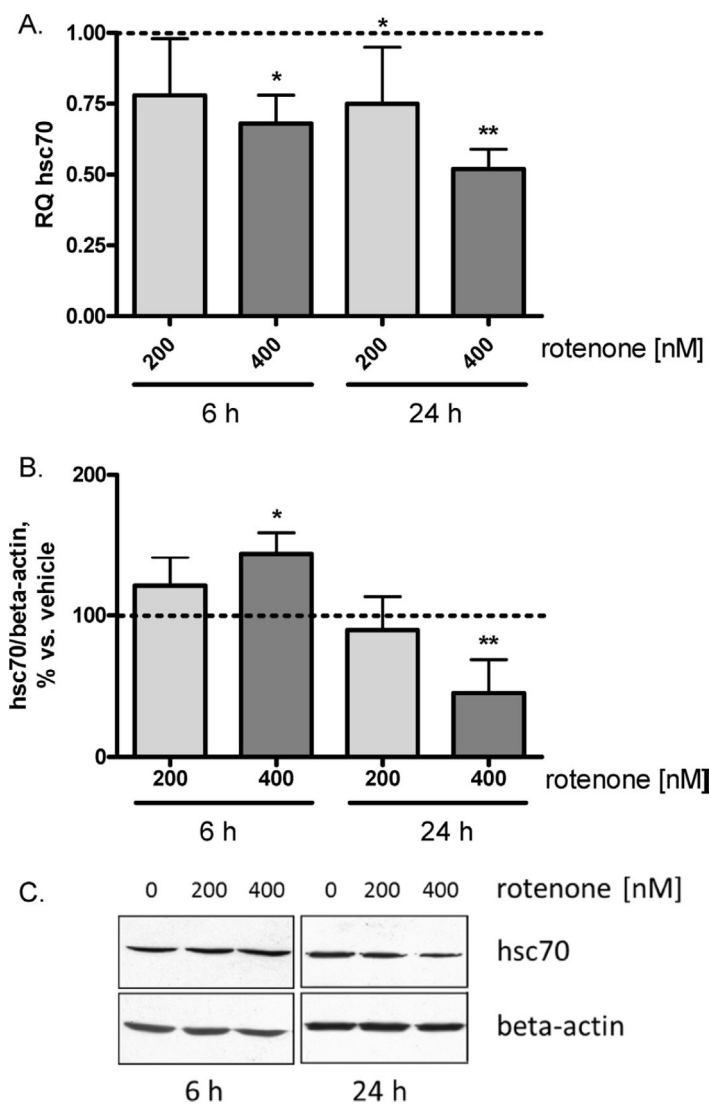


Figure 3

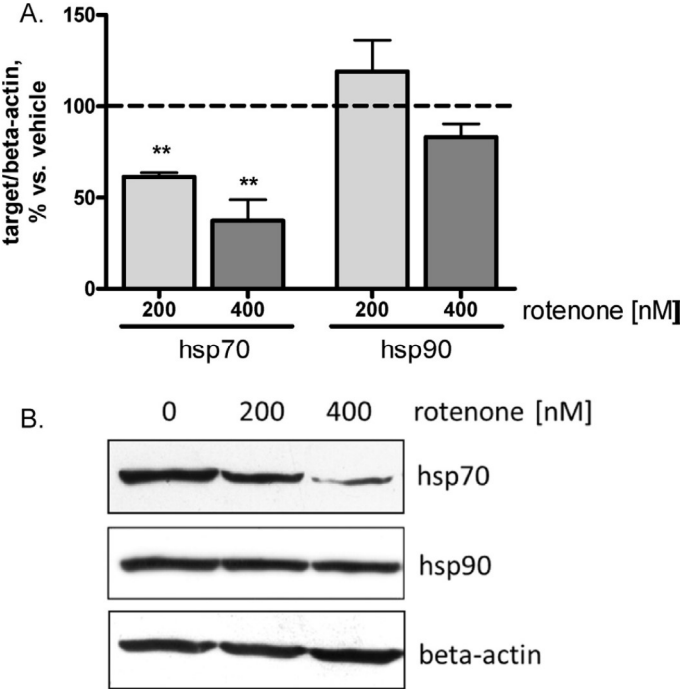


Figure 4

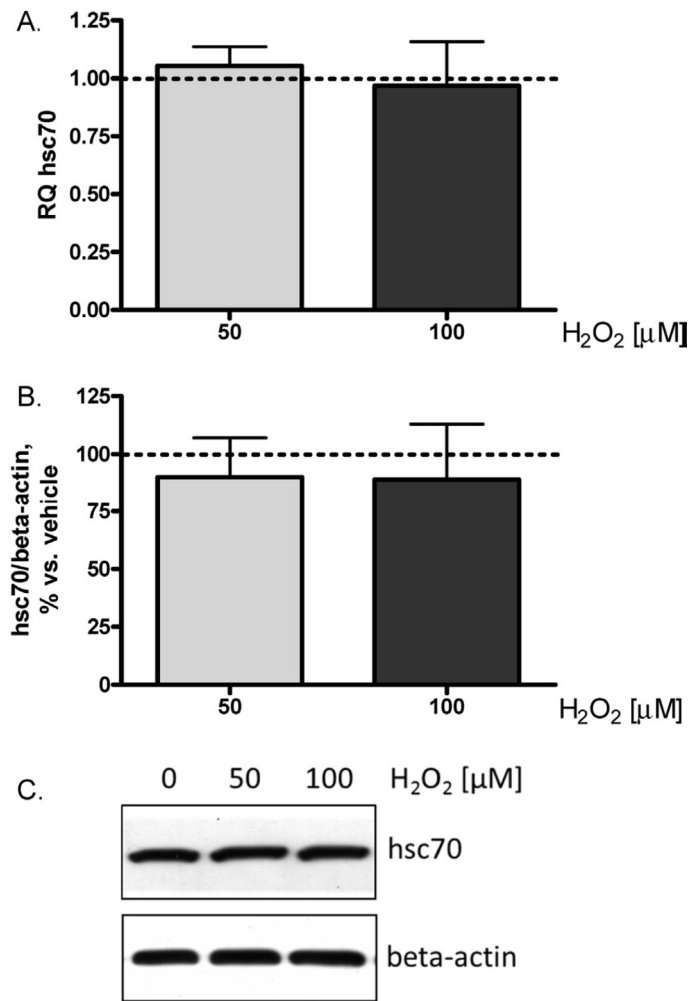


Figure 5

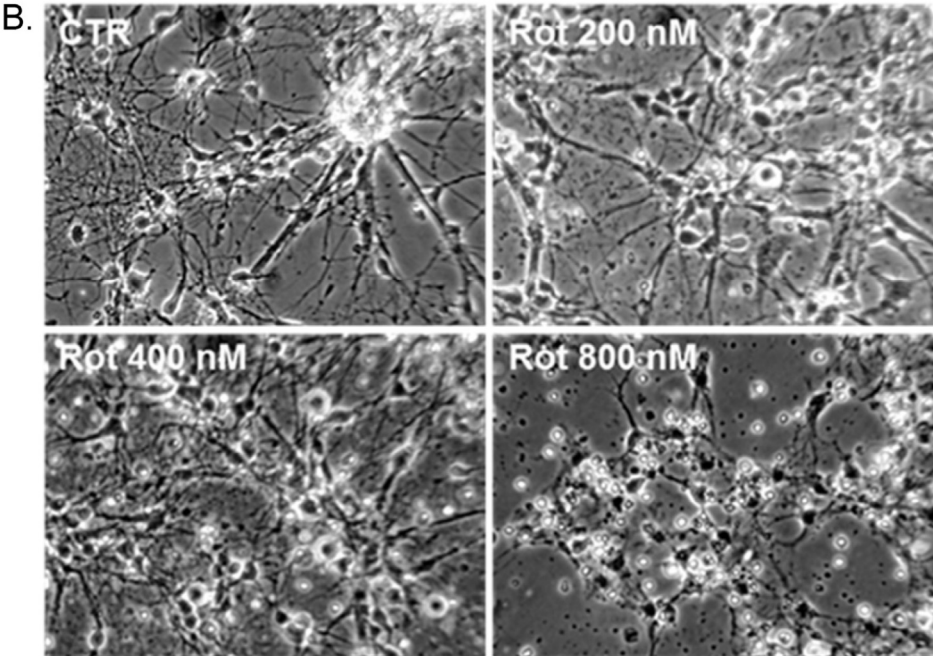
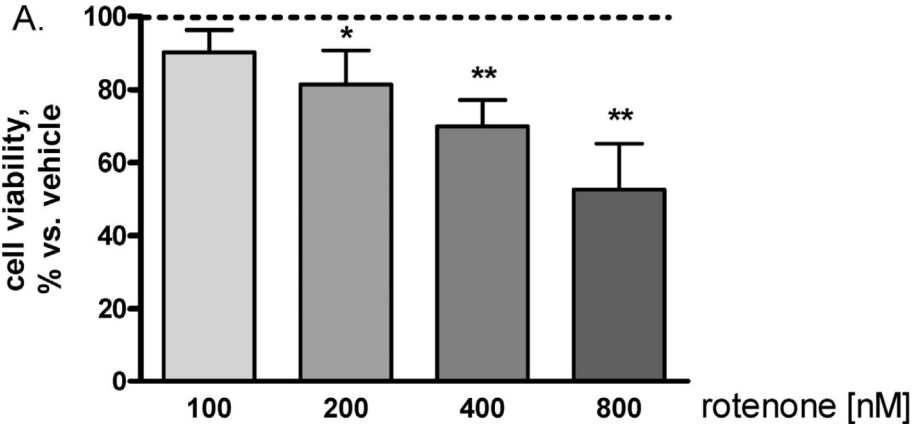


Figure 6

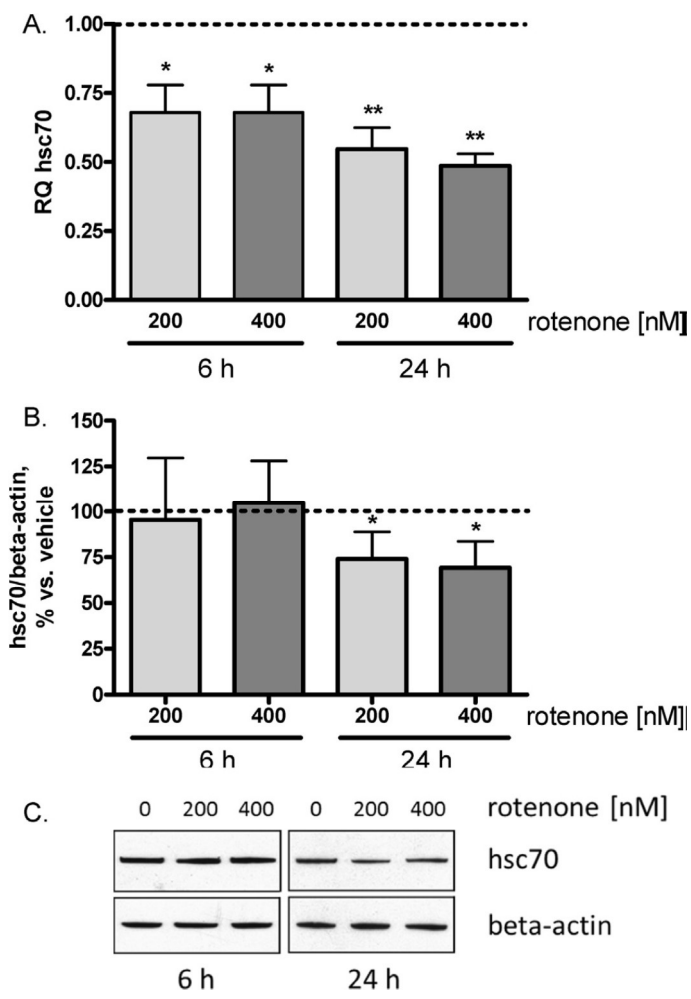


Figure 7

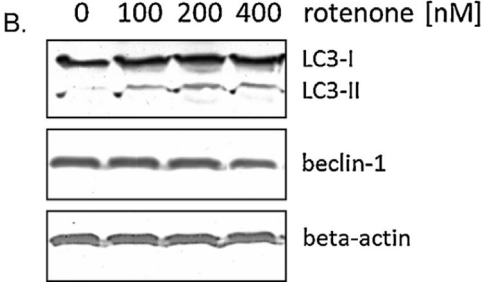
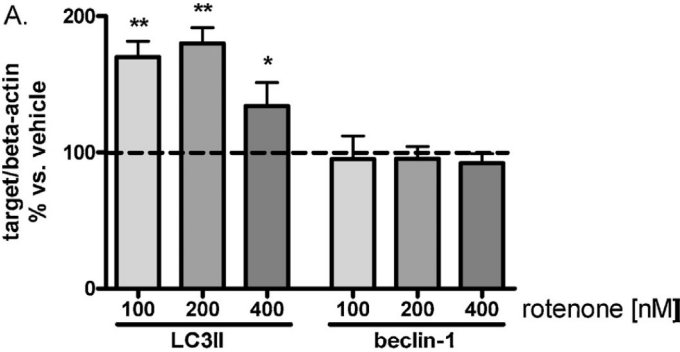


Figure 8

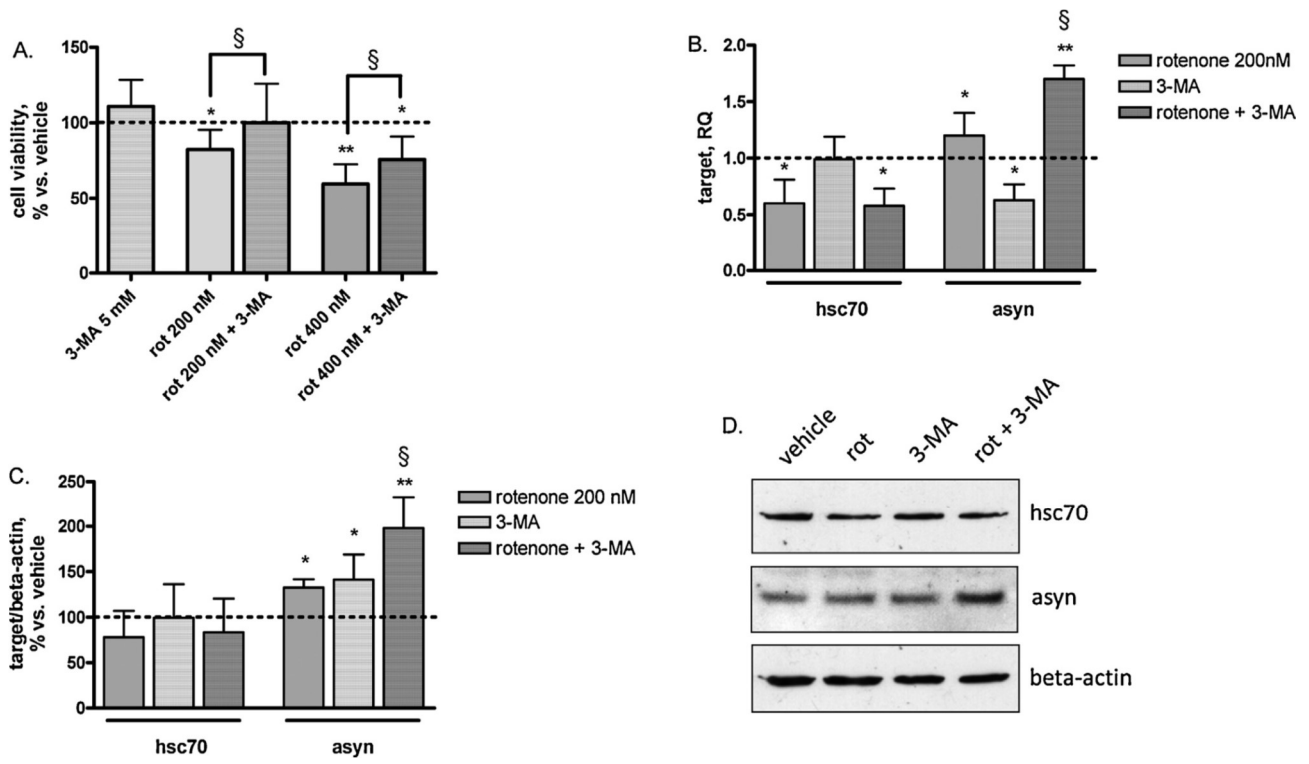


Figure 9

